

Band to Mott Insulator transition in the ionic Hubbard model

Philipp Brune, Arno P. Kampf

Angaben zur Veröffentlichung / Publication details:

Brune, Philipp, and Arno P. Kampf. 2002. "Band to Mott Insulator transition in the ionic Hubbard model." In High performance computing in science and engineering '01: transactions of the High Performance Computing Center Stuttgart (HLRS) 2001, edited by Egon Krause and Willi Jäger, 167-77. Berlin: Springer.

Nutzungsbedingungen / Terms of use:

licgercopyright

Dieses Dokument wird unter folgenden Bedingungen zur Verfügung gestellt: / This document is made available under the following conditions:

Deutsches Urheberrecht

Weitere Informationen finden Sie unter: / For more information see:

<https://www.uni-augsburg.de/de/organisation/bibliothek/publizieren-zitieren-archivieren/publizieren>



Band to Mott insulator transition in the ionic Hubbard model

Ph. Brune and A. P. Kampf

Theoretische Physik III, Elektronische Korrelationen und Magnetismus,
Institut für Physik, Universität Augsburg, 86135 Augsburg, Germany

Abstract. We investigate the ground state phase diagram of the one-dimensional “ionic” Hubbard model with an alternating periodic potential at half filling by numerical diagonalization of finite systems with the Lanczos and DMRG methods. In addition, we present results for the optical conductivity obtained by the recently developed dynamical DMRG (DDMRG) method. The band insulator to Mott insulator phase transition and its characteristics are discussed.

1 Introduction

The so-called “ionic” Hubbard model was originally proposed about 20 years ago in the context of organic charge transfer crystals consisting of a sequence of alternating donor (D) and acceptor (A) molecules ($\dots D^{+\rho} A^{-\rho} D^{+\rho} A^{-\rho}$) [1,2]. These stacks form quasi one-dimensional (1D) insulating or semiconducting chains, and are classified into two categories depending on the amount of charge transfer ρ : quasi-neutral for $\rho < 0.5$, and quasi-ionic for $\rho > 0.5$. Torrance *et al.* [1] found that several of these systems undergo a reversible neutral-to-ionic phase transition (NIT), i.e. a discontinuous jump in the ionicity ρ upon changing temperature or pressure. In a different context, the ionic Hubbard model has also been used recently to describe the ferroelectric transition in perovskite materials such as BaTiO_3 [4].

Explicitely, the 1D ionic Hubbard model is defined by the Hamiltonian

$$H = -t \sum_{i,\sigma} (1 + (-1)^i \delta) (c_{i\sigma}^\dagger c_{i+1\sigma} + h.c.) + U \sum_i n_{i\uparrow} n_{i\downarrow} + \frac{\Delta}{2} \sum_i (-1)^i n_i \quad , \quad (1)$$

where $c_{i\sigma}^\dagger$ creates an electron on site i with spin σ , $n_{i\sigma} = c_{i\sigma}^\dagger c_{i\sigma}$, U the on-site Hubbard interaction, Δ an on-site potential; in (1) we have included an additional Peierls modulation δ of the hopping matrix element t . The limit $\Delta = 0$ and $\delta > 0$ is called the *Peierls-Hubbard model*.

The NIT at finite temperatures has been intensively studied theoretically in a series of articles by Nagaosa *et al.* [2] using quantum Monte Carlo (QMC) simulations. NIT has been investigated. The 1D ionic Hubbard model (1) with $\Delta > 0$ and $\delta = 0$ at half filling has served as an appropriate model for

a D - A chain. The model parameters U and Δ in (1) are used for an effective description of the microscopic parameters, like e.g. the electron affinity of the acceptor molecules, the ionization potential of the donors, and the Madelung energy of ionized D^+A^- pairs. Within this picture, Δ could be interpreted as the energy necessary to move an electron from the donor to the acceptor.

For an understanding of the existence of a phase transition in the 1D ionic Hubbard model with $\delta = 0$ the best starting point is the atomic limit [8]. For $t = 0$, it is immediately seen that for half filling and $U < \Delta$ the ground state of (1) has two electrons on the B (i odd), and no electrons on the A sites (i even) ("neutral" phase). This corresponds to a charge density wave (CDW) ordering with maximum amplitude. On the other hand, for $U > \Delta$ each site is occupied by one electron ("ionic" phase). Obviously, for $t = 0$ a transition occurs at a critical value $U_C = \Delta$. This transition is expected to persist for $t > 0$, where the alternating potential still defines two sublattices A and B , opening up a band gap Δ for $U = 0$ at $k = \pm\pi/2$. For $t > 0$ the critical coupling shifts to $U_C(t) > \Delta$, with U_C monotonically increasing with increasing Δ . For $U, \Delta \gg t$ the system is close to atomic limit, and U_C approaches Δ from above.

For $U = 0$ the ground state at half-filling is a CDW band insulator (BI); its elementary excitation spectrum consists of particle-hole excitations over the band gap. We consider a system to be in a BI phase when the criterion $\Delta_S = \Delta_C$ holds where the spin (Δ_S) and the charge gap (Δ_C) are given by

$$\Delta_S = E_0(N = L, S_z = 1) - E_0(N = L, S_z = 0) \quad (2)$$

$$\Delta_C = E_0(N = L + 1, S_z = 0) + E_0(N = L - 1, S_z = 0) - 2E_0(N = L, S_z = 0) \quad (3)$$

$E_0(N, S_z)$ is the ground state energy, L the system length in units of the lattice constant, N the number of electrons in the system, and S_z the z -component of the total spin.

On the other hand, in the ionic phase for $U > U_C$ the charge gap is dominated by the Coulomb interaction U ; thus the system is a correlated insulator with $\Delta_C > \Delta_S$. However, in contrast to the cases with $\Delta = 0$ or $t = 0$, the CDW order is present in this phase for all finite values of U , except for $U \rightarrow +\infty$. If also $\Delta_S = 0$, i.e. if the system is a true Mott insulator (MI) or $\Delta_S > 0$, is an important question closely related to the physics of the intermediate region around $U \approx \Delta$, as well as the nature of the phase transition from the band to the correlated or Mott insulator.

The ionic Hubbard model is different from the Peierls-Hubbard model which is also a BI at $U = 0$, but in contrast to the ionic Hubbard model ($\delta = 0$) $\Delta_C > \Delta_S > 0$ is realized for any value $U > 0$, i.e. the phase transition from the Peierls BI to the correlated insulator occurs at $U_C = 0$.

2 Symmetry analysis

The Hamiltonian (1) for $\delta = 0$ is invariant with respect to *inversion* at a site i and *translation* by two lattice sites. Thus, any nondegenerate eigenstate of H is also an eigenstate of the operators that generate the corresponding symmetry transformation. We denote the site inversion operator by P , as defined by Gidopoulos *et al.* [8] through

$$Pc_{i\sigma}^\dagger P^\dagger = c_{L-i\sigma}^\dagger \quad \text{for } i = 0, 1, \dots, L-1. \quad (4)$$

Then, any nondegenerate eigenstate $|\psi_n\rangle$ of H must obey $P|\psi_n\rangle = \pm|\psi_n\rangle$. The alternating charge order (CDW) in the ground state at $U = 0$ will therefore persist up to $U \rightarrow +\infty$.

For $U = 0$, the ground state is a direct product of spin up and spin down Slater determinants, both formed from the same occupied spatial wavefunctions having the same parity $P_\sigma = \pm 1$, so the parity eigenvalue of the total wavefunction is given by their product $P = P_\downarrow \times P_\uparrow = 1$ for the two spin projections. Hence, the groundstate at $U = 0$ is even under site inversion. On the other hand, in the large U limit of the Hubbard model the mapping to the Heisenberg Hamiltonian can be used to show that for $L = 4n$ with periodic boundary conditions (PBC) or $L = 4n + 2$ with antiperiodic boundary conditions (APBC) the ground state obeys $P|\psi_0\rangle = -|\psi_0\rangle$ (for details see [8]). As a consequence, upon increasing the number of sites L , the ground state for $U \gg t$ will be odd with respect to P as long as $k = \pi/2$ is an allowed k value. This shows that for the ordinary Hubbard model the ground state has $P = +1$ only for $U = 0$, and $P = -1$ for any $U > 0$.

However, in the ionic Hubbard model ($\Delta > 0, \delta = 0$) the phase transition from a BI to a correlated insulator occurs at some finite $U_C > 0$. The site parity of the ground state remains even for all $U < U_C$ in the BI phase. At U_C , a ground state level crossing occurs, verified by exact diagonalization studies (see below), connected with a site parity change. Similar to the situation with $\Delta = 0$, for $U \gg t$ the ground state has odd site parity for $U > U_C$.

3 Lanczos exact diagonalization results

Using the Lanczos diagonalization method [12] the energies of the few lowest eigenstates were obtained for finite chains with $L = 4n$ and PBC or $L = 4n + 2$ with APBC. The purpose of these calculations was to extend earlier exact diagonalizations [5,8] for a better understanding of the symmetries of the eigenstates involved in the level crossing. We first analyze a short chain without a finite size scaling analysis. The thermodynamic limit will be addressed below by analyzing DMRG results.

In Fig. 1, the lowest eigenvalues of the ionic Hubbard model for $\Delta = 0.5t$, $L = 8$ and PBC are shown as a function of U . At $U = 1.3t$, a level crossing of the two lowest eigenstates occurs signaling a discontinuous phase transition.

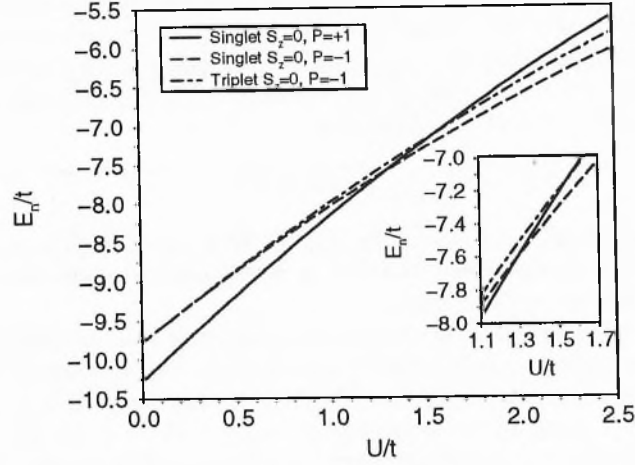


Fig. 1. Lowest energy eigenvalues of the ionic Hubbard model at half filling for $L = 8$ sites, periodic boundary conditions, $\Delta = 0.5t$, $\delta = 0$.

As pointed out before, a non-degenerate eigenstate of the ionic Hubbard model can only have site parity eigenvalues ± 1 , so the groundstate level crossing transition corresponds to a parity change.

For $U = \delta = 0$, the Hamiltonian (1) is easily diagonalized obtaining two energy bands $E_{1/2}(k) = \pm \sqrt{4 \cos^2(k) + (\Delta/4)^2}$. This is done by introducing new fermionic creation and annihilation operators $\{\gamma_{k\sigma b}^\dagger, \gamma_{k\sigma b}\}$ with an additional band index $b = 1, 2$ denoting the lower and upper bands, respectively. The first two degenerate excited states have negative site parity, because the ground state has positive parity and

$$P\gamma_{q\sigma 2}^\dagger\gamma_{q\sigma 1} = -\gamma_{q\sigma 2}^\dagger\gamma_{q\sigma 1}P \quad (5)$$

with $q = \pi/2$. The first two excited states shown in Fig. 1 are the spin singlet (total spin $S = 0$, $S_z = 0$) and triplet excitations ($S = 1$, $S_z = 0$) created from the ground state by applying the operators

$$\frac{1}{\sqrt{2}} \left(\gamma_{q\uparrow 2}^\dagger \gamma_{q\uparrow 1} - \gamma_{q\downarrow 2}^\dagger \gamma_{q\downarrow 1} \right) \quad , \quad \frac{1}{\sqrt{2}} \left(\gamma_{q\uparrow 2}^\dagger \gamma_{q\uparrow 1} + \gamma_{q\downarrow 2}^\dagger \gamma_{q\downarrow 1} \right) \quad . \quad (6)$$

Thus, both excited states have total momentum $k_{tot} = 0$ and negative site parity. For $U > 0$, these degenerate states split and the singlet state turns into the groundstate at U_c . Obviously, from symmetry considerations and exact diagonalizations of finite rings already a quite clear picture of the phase

diagram of the model emerges. At a finite $U_C > 0$ a level crossing phase transition occurs connected with a change of parity of the ground state.

4 DMRG results

Δ_C and Δ_S for longer chains have been calculated using the DMRG method [13,14]. In Fig. 2 extrapolated results are shown as a function of U . Calculations were performed with open boundary conditions (OBC) for $L = \{30, 40, 50, 60\}$ for all values of U (main figure), and additionally for $L = 200$ and $L = 300$ in the transition region around the estimated U_C (inset). In contrast to the definition (4), the charge gap in the DMRG calculations was obtained using

$$\Delta_C = \frac{1}{2} \left[E_0(N = L + 2, S_z = 0) + E_0(N = L - 2, S_z = 0) - 2E_0(N = L, S_z = 0) \right] \quad (7)$$

in order to calculate the energies E_0 in the subspace of total spin $S_z = 0$. We assume the finite size scaling behaviour to be of the form ($i \in \{S, C\}$) [15]

$$\Delta_i(L) = \Delta_i^\infty + \frac{A_i}{L} + \frac{B_i}{L^2} + \dots \quad , \quad (8)$$

which is the usual choice for extrapolations of data obtained with OBC.

The fact that the transition at U_C is connected with inversion symmetry requires some caution when open boundary conditions are used. In this case for $L = 2n$ the Hamiltonian (1) with $\delta = 0$ is not reflection symmetric at any site. Thus, the corresponding groundstate does not have a well defined site parity, and the level crossing transition does not occur. Instead, only a smooth crossover is observed. To overcome this problem, one might try to use chains with OBC and an *odd* number of sites $L = 2n + 1$, since the Hamiltonian in this case is reflection symmetric with respect to the central site, and a site parity operator is well defined by

$$P c_{i\sigma}^\dagger P = c_{L-1-i\sigma}^\dagger \quad . \quad (9)$$

The site parity eigenvalue of the $U = 0$ ground state for $L = 2n + 1$ is given by

$$P|\psi_0\rangle = (-1)^n |\psi_0\rangle \quad . \quad (10)$$

On the other hand, in the large U limit the mapping to the effective spin Hamiltonian could be used again. By extending the idea of Gidopoulos *et al.* [8] to chains with $L = 2n + 1$, for $U \gg t$ we obtain

$$P|\psi_0\rangle = (-1)^{\sum_{m=1}^{L-1} m} |\psi_0\rangle = (-1)^n |\psi_0\rangle \quad . \quad (11)$$

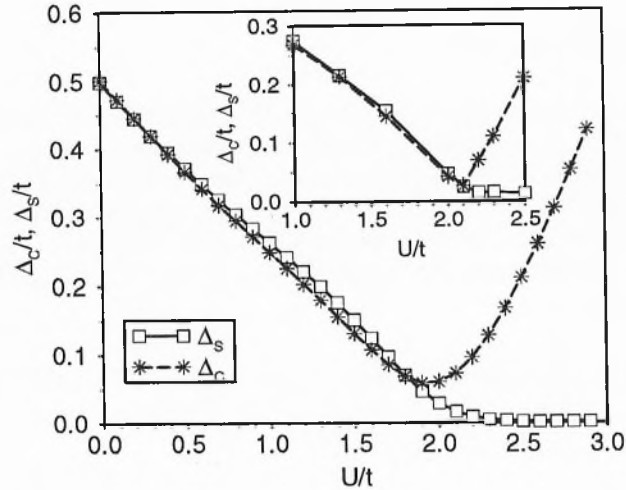


Fig. 2. Results for the spin (Δ_S) and charge (Δ_C) gap of the 1D ionic Hubbard model at half-filling with an on-site energy modulation $\Delta = 0.5t$ vs. U . Energies were obtained by DMRG calculations with $L = \{30, 40, 50, 60\}$ (main plot) and $L = \{30, 40, 50, 60, 200, 300\}$ (inset), and extrapolated to the infinite chain length limit.

Thus, the parity eigenvalue of the ground state is the same at $U = 0$ and $U \gg t$ for a given chain length, and no level crossing occurs. Thus we conclude that also for odd numbers of sites and OBC the level crossing in the ground state does not occur in finite chains.

Obviously, results for any choice of boundary conditions should recover the level crossing scenario when extrapolated to the thermodynamic limit. Due to the fact that the sharp transition at a well defined U_C does not exist in the finite chain results with OBC, the extrapolation is quite a subtle problem. This requires the use of very long chains in the critical region (up to $L = 300$ sites or more). As can be seen from the main plot in Fig. 2, extrapolating the results for $L = \{30, 40, 50, 60\}$ does not give a sharp transition behaviour of the gaps. Up to approximately $U \sim 0.4t$, the band insulator with $\Delta_C = \Delta_S$ persists, and for $U > 2.3t$ the system is a correlated insulator with $\Delta_C > \Delta_S > 0$. Within the numerical accuracy $\Delta_S = 0$, which suggests that this phase represents a true Mott insulator. The intermediate region does not show a clear sharp transition, the charge gap never closes, and one observes $\Delta_C \neq \Delta_S$ already below the estimated U_C .

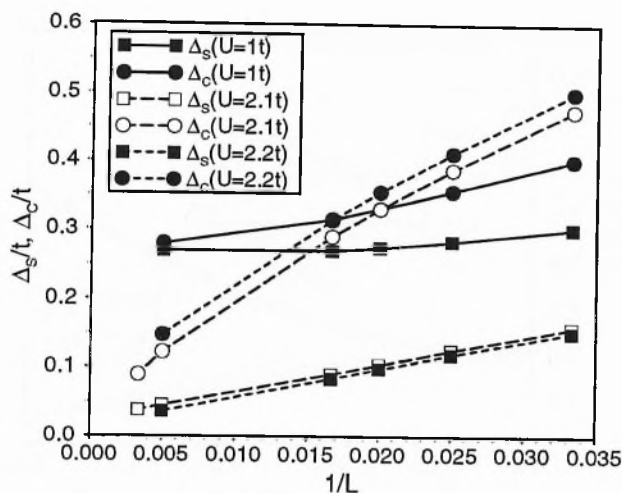


Fig. 3. Chain length dependence of the DMRG results for the spin (Δ_S) and charge (Δ_C) gap for $\Delta = 0.5t$ for selected values of U .

As illustrated in the inset, adding results for $L = 200$ and even $L = 300$ in the critical region changes the picture considerably, approaching the behaviour expected from the symmetry arguments and exact diagonalization results. This allows the conclusion that the above level crossing scenario will be recovered in the thermodynamic limit for the DMRG results on chains with an even number of sites. To illustrate the dependence of the gaps on the chain lengths L , a scaling plot for Δ_C and Δ_S at selected values of U as a function of $1/L$ is shown in Fig. 3. The changes in the behaviour occurring for longer chains are clearly visible. The DMRG calculations were performed with four finite lattice sweeps, and the number of states kept in the DMRG projection was increased from $m = 100$ to $m = 300$ during the sweeps. It becomes obvious, that DMRG studies requiring OBC can face problems when the transition under consideration is connected with a change in spatial symmetries broken by the OBC.

5 Optical Conductivity

To further analyze the band and correlated insulating phases we have calculated the frequency-dependent optical conductivity within the dynamical DMRG (DDMRG) approach making use of the Lanczos vector technique de-

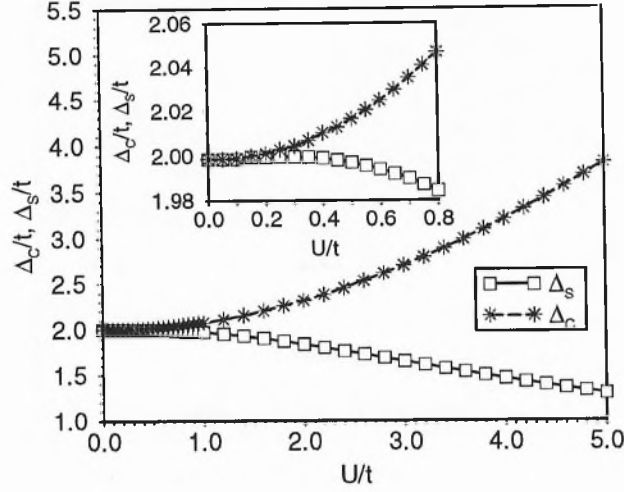


Fig. 4. Results for the spin (Δ_S) and charge (Δ_C) gap of the Peierls Hubbard model at half-filling with a modulation of the hopping amplitude $\delta = 0.1t$ as a function of the on-site Coulomb repulsion U . Energies were obtained by DMRG calculations with $L = \{30, 40, 50, 60\}$.

scribed in [16,17]. Calculations were performed for $L = 100$ sites with OBC using a Parzen filter to suppress the influence of the chain boundaries [17].

The real part of the longitudinal optical conductivity $\sigma(\omega)$ is determined by the linear response of the system to an external electromagnetic field. In the Kubo formalism, $\sigma(\omega)$ is connected to the imaginary part of the retarded current-current correlation function

$$\chi_{jj}(q, \omega) = \frac{i}{La} \int_0^\infty d\tau e^{i\omega\tau} \langle \psi_0 | [j_{-q}(\tau), j_q(0)] | \psi_0 \rangle, \quad (12)$$

with a the lattice constant and $|\psi_0\rangle$ denoting the exact groundstate of (1). For $\omega > 0$ the imaginary part of χ_{jj} can be obtained numerically from [19]

$$\text{Im} \chi_{jj}(q, \omega) = -\text{Im} \frac{\hbar}{La} \langle \psi_0 | j_q \frac{1}{\hbar\omega + E_0 - H + i0^+} j_q | \psi_0 \rangle. \quad (13)$$

Here, the current operator is defined by

$$j_q = -it \frac{ea}{\hbar} \sum_{i,\sigma} e^{iqx_i} (c_{i+1\sigma}^\dagger c_{i\sigma} - c_{i\sigma}^\dagger c_{i+1\sigma}) , \quad (14)$$

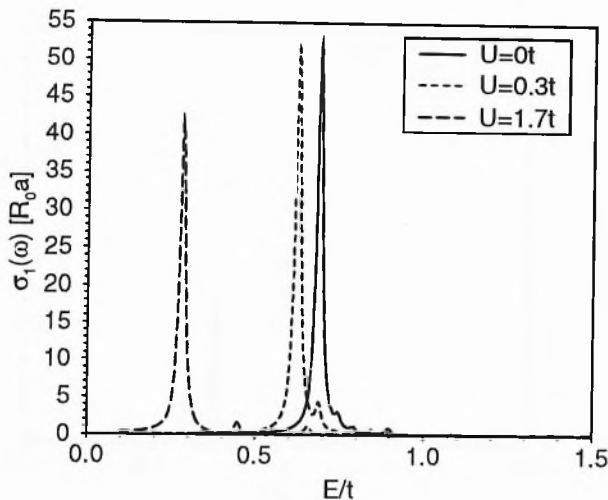


Fig. 5. Real part of the optical conductivity $\sigma_1(\omega)$ in units of $R_0 a = e^2 a / \hbar$ vs. energy $E = \hbar \omega$ for the half-filled 1D ionic Hubbard model with on-site energy modulation $\Delta = 0.5t$. A finite broadening $\eta = 0.01t$ of the peaks has been used. The selected values of the on-site Coulomb repulsion U shown all lie within the band insulating phase ($U < U_C$). The results were obtained by DDMRG calculations using the Lanczos vector method for a chain with $L = 100$ sites and open boundary conditions.

where e is the electron charge. The real part of the optical conductivity for $q = 0$ is then given by

$$\sigma_1(\omega) = D\delta(\omega) + \sigma_1^{reg}(\omega > 0) = D\delta(\omega) + \frac{1}{\hbar\omega} \text{Im}\chi_{jj}(q=0, \omega) \quad (15)$$

For the band and correlated insulating phases we always have a vanishing Drude weight $D = 0$.

In Fig. 5 DDMRG results for $\sigma_1(\omega)$ are plotted for $\Delta = 0.5t$ and different values of $U < U_C$ in the band insulator phase. In the infinite chain for $U = 0$ $\sigma_1(\omega)$ vanishes below the band gap Δ , and diverges as $\sigma_1(\omega) \sim \frac{1}{\sqrt{\omega - \Delta}}$ for $\omega \rightarrow \Delta$ [18]. This divergence is anticipated by the very strong dominant lowest excitation peak in the finite chain results. The picture does not change qualitatively upon increasing U over the whole band insulator phase. It suggests that the physics of the excitations in the band insulating phase remains similar to $U = 0$ for any finite $U < U_C$.

For $U > U_C$, the situation is different, as demonstrated in Fig. 6. There we show the DDMRG result for $\sigma_1(\omega)$ for $U = 2.9t$, with the other parameters

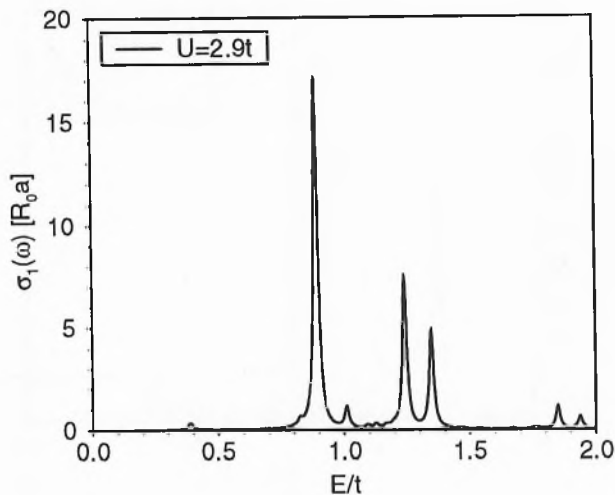


Fig. 6. Same as Fig. 5, but for a value of U corresponding to the correlated insulating phase ($U > U_C$).

as in Fig. 5. Here, the properties of the charge excitations are expected to be similar to the Hubbard model where $\sigma_1(\omega) \sim \sqrt{\omega - \Delta_C}$ near the charge gap Δ_C [19].

Due to the strong finite size effects, the square root behaviour itself is not visible in Fig. 6, but the lowest energy peak of $\sigma_1(\omega)$ is clearly not the one with the highest spectral weight anymore. Instead, the spectral weight increases with ω above the gap, and decreases again after reaching a maximum value. The qualitative behaviour is consistent with the results obtained for the Hubbard chain at $U = 3t$ [19].

Whenever the site parity of an eigenstate is well defined quantity, the current operator $j_{q=0}$ will change parity when acting on that state. Thus, the matrix element $\langle \psi_n | j_{q=0} | \psi_0 \rangle$ in (12) vanishes whenever $|\psi_n\rangle$ and $|\psi_0\rangle$ have the same parity. In the ionic Hubbard model, the first two excited states have parity opposite to the ground state, and the singlet state contributes to the optical conductivity. Precisely at U_C , the ground state and the first excited state cross, so the ground state is degenerate. This critical point has been commonly referred to in the literature as “metallic”, due to the vanishing charge gap $\Delta_C = 0$. This implies the existence of optical excitations at arbitrary small energies $\omega > 0$. However, per definition a metal is characterized not only by gapless excitations, but also by a finite Drude weight $D > 0$, i.e. a finite dc conductivity. Thus, it follows that the ionic Hubbard model

for $U = U_C$ has a gapless optical spectrum, but it cannot be considered “metallic” in the usual sense.

6 Conclusions

References

1. J. B. Torrance *et al.*, Phys. Rev. Lett. **46**, 253 (1981); *ibid.* **47**, 1747 (1981).
2. N. Nagaosa and J. Takimoto, J. Phys. Soc. Jpn. **55**, 2735, 2747 (1986); N. Nagaosa, *ibid.* **55**, 2754 (1986).
3. A. Girlando and A. Painelli, Phys. Rev. B **34**, 2131 (1986).
4. T. Egami, S. Ishihara, M. Tachiki, Science **261**, 1307 (1993).
5. R. Resta and S. Sorella, Phys. Rev. Lett. **74**, 4738 (1995).
6. G. Ortiz *et al.*, Phys. Rev. B **54**, 13515 (1996).
7. M. Fabrizio *et al.*, Phys. Rev. Lett. **83**, 2014 (1999).
8. N. Gidopoulos, S. Sorella, and E. Tosatti, Eur. Phys. J. B **14**, 217 (2000).
9. Y. Takada and M. Kido, J. Phys. Soc. Jpn. **70**, 21 (2001).
10. T. Wilkens and R. M. Martin, preprint cond-mat/0007472 (2000).
11. Y. Anusooya-Pati *et al.*, preprint cond-mat/0009153 (2000).
12. C. Lanczos, J. Res. Natl. Bur. Stand. **45**, 255 (1950).
13. S. R. White, Phys. Rev. Lett. **69**, 2863 (1992); Phys. Rev. B **48**, 10345 (1993).
14. I. Peschel *et al.*, (Eds.): *Density-Matrix Renormalization*, Springer (1999).
15. R. Noack, private communication.
16. K. A. Hallberg, Phys. Rev. B **52**, R9827 (1995).
17. T. D. Kühner and S. R. White, Phys. Rev. B **60**, 335 (1999).
18. F. Gebhard *et al.*, Phil. Mag. B **75**, 1, 13, 47 (1997).
19. E. Jeckelmann *et al.*, Phys. Rev. Lett. **85**, 3910 (2000).